Journal of Economic Dynamics & Control 146 (2023) 104561

Contents lists available at ScienceDirect

Journal of Economic Dynamics & Control

journal homepage: www.elsevier.com/locate/jedc

Unstable diffusion in social networks☆

Teruyoshi Kobayashi[a,*], Yoshitaka Ogisu[b], Tomokatsu Onaga[c]

[a] Department of Economics, Center for Computational Social Science, Kobe University, Kobe, Japan
[b] Graduate School of Economics, Kobe University, Kobe, Japan
[c] Frontier Research Institute for Interdisciplinary Sciences, Graduate School of Information Sciences, Tohoku University, Sendai, Japan

ARTICLE INFO

Article history:
Received 16 May 2022
Revised 9 September 2022
Accepted 31 October 2022
Available online 3 November 2022

JEL classification:
C72
D85
L14

Keywords:
Social network
Diffusion
Coordination game
Mean-field method
Master equations

ABSTRACT

How and to what extent will new activities spread through social ties? To answer this question, we present an analytical framework that allows us to describe the diffusion dynamics on complex networks more accurately than the conventional mean-field approach. Based on two classes of network games, we find that the spread of multiple activities is expressed as a saddle path, and thus, inherently unstable. In particular, when the two activities are sufficiently substitutable, either of them will dominate the other by chance even if they are equally attractive *ex ante*. We argue that, in environments where such symmetry-breaking occurs, any average-based approximation method may not correctly capture the Nash equilibrium — the steady state of an actual diffusion process.

1. Introduction

Social activities, new ideas, and innovative technologies spread through networks of social ties formed by friends, colleagues, and followers on social media such as Facebook, Twitter, and Instagram. Social ties (in physical and online spaces) are not only a channel through which information flows, but also propagate influence. For example, an individual's decision regarding which activities to join often depends on the fraction and/or the number of friends participating in the activities. If the majority of friends already joined a certain activity, then that activity would be more attractive to that individual than the activities not popular among friends. The contagious aspect of peer effects through social ties has been extensively studied in models of coordination games on networks (Jackson, 2008; Jackson and Zenou, 2015; Kreindler and Young, 2014; Morris, 2000; Young, 2011), in which they examine the effect of network structure on the possibility of cascades. Another framework is based on a utility-maximization problem that incorporates gains from interacting with adjacent players (Ballester et al., 2006; Chen et al., 2018). They prove that equilibrium strategies are determined by the players' positions in the network characterized by their Bonacich centralities (Bonacich, 1987).

☆ Kobayashi acknowledges financial support from JSPS KAKENHI 19H01506, 20H05633 and 22H00827. Onaga acknowledges financial support from JSPS KAKENHI 19K14618, 19H01506 and 22H00827. We would like to thank Takashi Shimizu, who provided valuable comments on an earlier version of this paper.

* Corresponding author.
E-mail address: kobayashi@econ.kobe-u.ac.jp (T. Kobayashi).

https://doi.org/10.1016/j.jedc.2022.104561

In standard 2×2 coordination games with a single activity (or product, convention, opinion, whatever), the players' decisions are binary (e.g., do it or do not do it). However, when there are two competing activities, denoted by A and B, the payoff matrix generally becomes 4×4 and each player's option is no longer binary; there are four pure strategies in the strategy set $\{00, 01, 10, 11\}$,[1] where "00" denotes the strategy of not joining either activity (or the status quo), "01" (resp. "10") denotes the strategy of joining activity A only (resp. B only), and "11" denotes the *bilingual option* of joining both A and B (Arigapudi, 2020; Oyama and Takahashi, 2015).[2] The presence of multiple activities allows us to study richer dynamics compared to the binary cascade models. First, while there is only one type of strategic shift in the diffusion of a single activity (i.e., $00 \to 01$), there are multiple patterns of strategic shifts, e.g., $01 \to 10$, $01 \to 11$, $10 \to 11$, etc, which simply expands the set of possible paths to an equilibrium. Second, we can introduce the reversibility of strategic choices; players may revert their strategies, e.g., $01 \to 10 \to 01$, in response to changes in the neighbors' states. The propagation process is thus no longer monotonic, where an activity may spread temporarily but fade away to be replaced by the other activity, while diffusion is always monotonic in the binary cascade models.[3] Third, the diffusion process can be more stochastic especially when the two activities are equally attractive. In complex networks, whose structures are far from regular and symmetric, the influence of initially active players is highly heterogeneous. Thus, the popularity of an activity in the terminal state will be strongly affected by the extent to which the activity spreads in the early stage of diffusion.

When the network structure is complex, unlike regular lattices, star graphs, and circular networks, it is notoriously difficult to calculate the Nash equilibrium in an exact manner even in binary games. In the literature, it is common to calculate the Nash equilibrium using a *mean-field* (MF) approximation (Jackson and Yariv, 2007; Lelarge, 2012; López-Pintado, 2008; 2012; Sadler, 2020), assuming that players are sufficiently homogeneous such that the probability of each player being in a given state can be well approximated by the corresponding average over all players. However, Gleeson and Porter (2018) and Kobayashi and Onaga (2022) quantitatively verify that the MF approximation can be inaccurate, especially when the network connectivity is close to the critical points at which the size of cascades changes drastically. They show that a *message-passing approach* is always more precise than the conventional MF approximation and that an iteration algorithm surely converges to a fixed point that corresponds to the simulated Nash equilibrium.

In this study, we examine two classes of games that describe multiple-activity diffusion on complex networks: i) coordination games with multiple activities, also known as *bilingual games* (Goyal and Janssen, 1997; Immorlica et al., 2007; Kobayashi, 2022; Oyama and Takahashi, 2015), and ii) the utility-based games on networks proposed by Ballester et al. (2006) and Chen et al. (2018). A common property of the two classes of games is that the optimal strategic choices are given by a set of threshold rules: *fractional threshold rules* (Watts, 2002) in coordination games, and *absolute threshold rules* (Granovetter, 1978) in the utility-based games. In each of these classes, we calculate the Nash equilibrium highly accurately by solving a system of differential equations, called the *approximate master equations* (AME) (Gleeson, 2011; 2013). The key benefit of analyzing with a system of differential equations is that it gives us the dynamical path of the popularity of each activity, i.e., the extent to which each activity spreads over the network at any given point in time.

The main results are summarized as follows. First, the system of equations given by the AME approach reveals the diffusion dynamics of multiple activities highly accurately in the sense that the calculated paths well match the simulated diffusion processes and correctly predict the Nash equilibrium. On the other hand, the MF equations, while they are simpler and more analytically tractable, replicate the simulated paths only roughly, and the predicted Nash equilibria can deviate from the simulated ones.

Second, we find that there are four distinct regimes characterized by different Nash equilibria, depending on the relative attractiveness of the activities and connectivity of the network. At the boundary of these regimes, a slight change in the relative attractiveness or network connectivity may drastically shift the equilibrium, a phenomenon called *phase transition* (Gai and Kapadia, 2010; Watts, 2002). Thus, a small change in the attractiveness and/or the network structure may initiate or terminate the widespread diffusion of an activity. This suggests that the diffusion dynamics are unstable at the critical points, and the popularity of an activity is far from proportional to its intrinsic attractiveness.

Third, except at those boundaries, the diffusion dynamics are stable and the equilibrium is highly predictable when the two activities are complementary or neutral. However, this is not necessarily the case when they are substitutes. Suppose that the two activities are perfectly symmetric in the sense that their attractiveness is represented by exactly the same payoff/preference parameters. In theory, we always obtain a common solution for the cascade sizes of symmetric activities, e.g., 40% of the population adopts activity A and the remaining 40% adopts activity B, because there is no factor that differentiates between the two, at least on average. In fact, this is not necessarily the case in the simulated diffusion processes. The analytical solutions would indeed be correct if the topological properties of the initially active players (i.e., *seed nodes*) are symmetric, but such a situation rarely occurs in complex networks. Our numerical experiments reveal that diffusion processes on complex networks generated from the same degree distribution can still reach totally different Nash equilibria when the two activities are substitutes. This suggests that equally-attractive yet substitutable activities do not necessarily gain equal popularity, and either activity may even dominate the other through the cascade of peer effects.

[1] The strategies are labeled in the order of the binary number system.

[2] In Oyama and Takahashi (2015) and Arigapudi (2020), the strategy "00" (i.e., do-nothing strategy) is not considered, and each player selects either or both of the two activities. In our study, the strategy "00" is the status quo for all players except the *seed players* that are initially activated.

[3] Note that the standard binary cascade models do not exhibit such a non-monotonic behavior, allowing us to prove the stability of an equilibrium and convergence of an iteration algorithm (Jackson and Yariv, 2007; Kobayashi and Onaga, 2022).

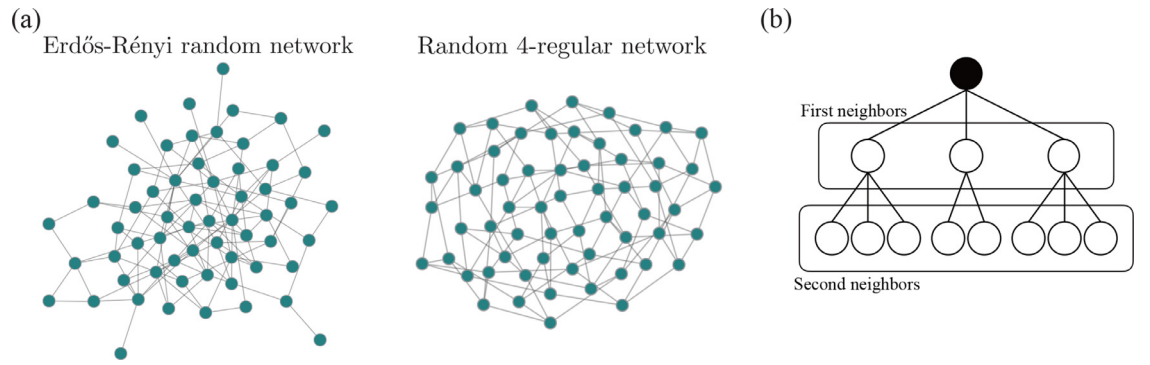

Fig. 1. Structure of random networks. (a) Visualization of Erdős-Rényi random networks and random z-regular networks. $N = 60$ and $z = 4$ in both cases. (b) Schematic of a tree-like structure.

The possibility of *symmetry breaking* also raises an important issue for theoretical studies of network games. With such an unstable equilibrium, any deterministic equilibrium would fail to predict the "true" Nash equilibrium since one of the possible equilibria will inevitably be achieved by chance, depending on the details of network structure that cannot be captured by the degree distribution. Symmetry breaking has long been recognized as a source of diversity in economic development (Acemoglu et al., 2017; Matsuyama, 2002), financial globalization (Matsuyama, 2004), and international trade (Chatterjee, 2017; Matsuyama, 2013). To the best of our knowledge, this is the first study that shows why almost equally attractive activities (or technologies, products, etc) can gain totally different levels of popularity.

2. Diffusion through coordination games

2.1. Network structure

Let us consider synthetic networks formed by N players, where N is assumed to be sufficiently large. Player i is connected to k_i other players by undirected and unweighted edges. k_i is called the *degree* of player i (or node i). Players at the end of the edges emanating from i are called *neighbors* of player i. For a given average degree z, we consider a whole ensemble of many possible networks in a given class, where a particular network structure is realized with a certain probability. That is, we do not focus on a particular single network, rather we specify the distribution of all possible network structures that would appear in a given network model. Any realized network is, therefore, an instance drawn from the ensemble uniformly at random. Examples of Erdős-Rényi networks (Erdős and Rényi, 1959) and random regular graphs are shown in Fig. 1a. Basic properties of Erdős-Rényi networks are described in Section S1 in the Online Appendix.

While we use Erdős-Rényi networks and random z-regular graphs (Fig. 1a) in our analysis, the only network property required for our approach is a locally tree-like structure in which local cycles can be ignored (Fig. 1b). For instance, Erdős-Rényi networks are locally tree-like as long as the connecting probability $q = z/(N-1)$ is sufficiently small (i.e., $z \ll N$).[4] A more general class of network models, called the *configuration models*, in which the degree distribution is prespecified while nodes are connected at random subject to the degree constraint, also exhibit a locally tree-like property (Molloy and Reed, 1995; Newman, 2018). Clearly, Erdős-Rényi random networks and z-regular networks are special cases of the configuration model; the degree distributions q_k for these networks are respectively given by $q_k = z^k e^{-z}/k!$ and $q_z = 1$.

2.2. Coordination games with a bilingual option

Throughout the paper, we consider two types of activities, denoted by A and B. Players will benefit from an activity if they enjoy the same activity as their neighbors. The two activities may be complements (e.g., drinking and smoking), substitutes (e.g., committing a crime and taking higher education), or neutral. For each of the two activities, players face a binary problem for which they adopt either action 0 ("don't do it") or action 1 ("do it"). The strategy set is thus given by $\{00, 01, 10, 11\} \equiv S$. Strategy 11 is called the *bilingual option* where the player engages in both activities (Arigapudi, 2020; Kobayashi, 2022; Oyama and Takahashi, 2015). Each player selects a pure strategy $s \in S$, taking all the neighbors' strategies as given.

2.2.1. Pure strategy equilibria in a bilateral game

The payoff matrix of the 4×4 bilateral coordination game is given in Tab. 1. A player receives payoff $a > 0$ (resp. $b > 0$) of coordinating with a neighbor if they both join activity A (resp. B). The cost of participating in an activity is given by c,

[4] See Newman (2018) ch. 12 for the property of the tree-like structure.

Table 1
Payoff matrix of a coordination game with multiple activities. The two activities are complements (resp. substitutes) when $\delta > 0$ (resp. $\delta < 0$).

	00	01	10	11
00	0,0	$0, -c$	$0, -c$	$0, -2c$
01	$-c, 0$	$a-c, a-c$	$-c, -c$	$a-c, a-2c$
10	$-c, 0$	$-c, -c$	$b-c, b-c$	$b-c, b-2c$
11	$-2c, 0$	$a-2c, a-c$	$b-2c, b-c$	$a+b+\delta-2c, a+b+\delta-2c$

where $0 < c < a$ and $c < b$, so the net payoff of coordinating on activity A (resp. B) leads to $a - c > 0$ (resp. $b - c > 0$). If two players successfully coordinate on both activities, both players receive $a + b$ plus extra payoffs δ, for a total net payoff of $a + b + \delta - 2c$. δ represents the degree of complementarity between the two activities; $\delta > 0$ (resp. $\delta < 0$) when the two activities are complementary (resp. substitutes).[5] Note that if $a + b + \delta - 2c > a - c$ and $a + b + \delta - 2c > b - c$, which are satisfied when $\delta > c - b$ and $\delta > c - a$, then the pure-strategy Nash equilibria are given by $(00, 00)$, $(01, 01)$, $(10, 10)$, and (11,11), and (11,11) is also the Pareto dominant equilibrium.

Proposition 1. *Suppose that $a > c$, $b > c$, $\delta > c - a$, and $\delta > c - b$. The strategy pair (11,11) is the Pareto dominant Nash equilibrium, and the (pairwise) risk dominant equilibrium is*

$$\begin{cases} (00, 00) & \text{if} \quad c - \delta < a < 2c, \ c - \delta < b < 2c, \ \text{and } a + b + \delta < 4c, \\ (01, 01) & \text{if} \quad 2c < a, \ a > b, \ \text{and } c < b < 2c - \delta, \\ (10, 10) & \text{if} \quad 2c < b, \ b > a, \ \text{and } c < a < 2c - \delta, \\ (11, 11) & \text{if} \quad 2c - \delta < a, \ 2c - \delta < b, \ \text{and } a + b + \delta > 4c. \end{cases} \tag{1}$$

Proof. It is obvious that the strategy pair (11,11) is Pareto dominant. To obtain a risk dominance equilibrium, consider subgames restricted to two strategies. For (01,01) to be risk dominant, for instance, (01,01) has to risk dominate all the other Nash equilibria: (00,00), (10,10) and (11,11) (Harsanyi and Selten, 1988; Young, 1993). Under the assumptions that $a > c$, $b > c$, $\delta > c - a$ and $\delta > c - b$, we have the following conditions of (strict) risk dominance for each subgame:

$$\text{(01,01) risk dominates} \begin{cases} (00, 00) & \text{if } a > 2c, \\ (10, 10) & \text{if } a > b, \\ (11, 11) & \text{if } b < 2c - \delta, \end{cases} \tag{2}$$

$$\text{(10,10) risk dominates} \begin{cases} (00, 00) & \text{if } b > 2c, \\ (11, 11) & \text{if } a < 2c - \delta, \end{cases} \tag{3}$$

$$\text{(11,11) risk dominates } (00, 00) \text{ if } a + b + \delta > 4c. \tag{4}$$

The conditions (2)–(4), combined with the four assumptions, define pairwise risk-dominant equilibria depending on the relative sizes of the parameters, as presented in (1). □

When δ is negative and large in absolute value such that $\delta < c - a$ or $\delta < c - b$, the action pair (11,11) is no longer a Nash equilibrium since joining both activities is not beneficial. In the following analysis, we employ the assumption that $\delta > c - a$ and $\delta > c - b$ to focus on the situation in which the bilingual option can be an equilibrium strategy.

Assumption 1. $\delta > c - a$ and $\delta > c - b$.

2.2.2. Multilateral games with k neighbors

In games with k neighbors, the total payoffs of a player are given by the sum of the payoffs received in the k bilateral games. Let $v(s, \mathbf{m})$ denote the total payoffs of a player who adopts strategy $s \in S$ and faces the neighbors' strategy profile $\mathbf{m} = (m_{00}, m_{01}, m_{10}, m_{11})^\top$, where $m_s \in \mathbb{Z}_{\geq 0}$ denotes the number of neighbors that adopt strategy $s \in S$. Note that we have $\sum_{s \in S} m_s = k$ for nodes with degree k. For a given $\mathbf{m}$, the payoff of each strategy leads to

$$v(00, \mathbf{m}) = 0, \tag{5}$$

$$\begin{aligned} v(01, \mathbf{m}) &= -c(k - m_{01} - m_{11}) + (a - c)(m_{01} + m_{11}) \\ &= -ck + a(m_{01} + m_{11}), \end{aligned} \tag{6}$$

[5] In Oyama and Takahashi (2015), they consider an extra cost of taking a bilingual option, which needs to be incurred independently of the other player's response. In the current payoff structure, we do not consider such an extra cost, where the cost of taking a bilingual option is given by the sum of the costs for each action. Instead, we introduce an extra payoff, δ, of coordinating on the bilingual option.

$$v(10,\mathbf{m}) = -ck + b(m_{10} + m_{11}), \tag{7}$$

$$v(11,\mathbf{m}) = -2ck + am_{01} + bm_{10} + (a+b+\delta)m_{11}. \tag{8}$$

The optimal strategy s^* for a given $\mathbf{m}$, is then given by

$$s^*(\mathbf{m}) = \arg\max_{s\in S} v(s,\mathbf{m}). \tag{9}$$

Since $v(00,\mathbf{m}) = 0$, players adopt strategies other than 00 if the total payoffs of those strategies are positive.[6] The conditions for $v(01,\mathbf{m}) > 0$ and $v(10,\mathbf{m}) > 0$ are given by the following simple threshold rules:

$$v(01,\mathbf{m}) > 0 \quad \text{iff} \quad \frac{m_{01}+m_{11}}{k} > \frac{c}{a}, \tag{10}$$

$$v(10,\mathbf{m}) > 0 \quad \text{iff} \quad \frac{m_{10}+m_{11}}{k} > \frac{c}{b}. \tag{11}$$

It should be noted that if there were only one activity, say activity A, the players' behavior would be ruled by a *fractional threshold rule*, i.e., $m_{01}/k > c/a$, as in the well-studied models of contagion (Jackson, 2008; Morris, 2000; Watts, 2002), in which each player adopts either strategy 00 or 01. Since we have a bilingual option here, the optimal strategy is not determined simply by the two conditions (10) and (11).

The conditions $v(11,\mathbf{m}) > v(01,\mathbf{m})$ and $v(11,\mathbf{m}) > v(01,\mathbf{m})$ are respectively rewritten as

$$v(11,\mathbf{m}) > v(01,\mathbf{m}) \quad \text{iff} \quad \frac{m_{10}}{k} + \left(1+\frac{\delta}{b}\right)\frac{m_{11}}{k} > \frac{c}{b}, \tag{12}$$

$$v(11,\mathbf{m}) > v(10,\mathbf{m}) \quad \text{iff} \quad \frac{m_{01}}{k} + \left(1+\frac{\delta}{a}\right)\frac{m_{11}}{k} > \frac{c}{a}. \tag{13}$$

Suppose for the moment that $\delta > 0$. Conditions (11) and (12) indicate that the fraction of neighbors joining activity B needed for strategy 11 to be preferable to strategy 01 will be less than that required for strategy 10 to be preferable to strategy 00. This is because when $\delta > 0$, the payoff of engaging in both activities is greater than the sum of the payoffs of each activity. However, if the two activities are substitutes, and thereby $\delta < 0$, the benefit of joining an additional activity is diminished, so the condition for joining activity B *in addition to* A will be more stringent than condition (11), which is the condition for deciding whether to participate in B or do nothing. The same argument also holds for the relationship between $v(11,\mathbf{m})$ and $v(10,\mathbf{m})$ (Eq. 13).

A crucial difference from the bilateral coordination games is that in this multilateral environment, coordinating with neighbors may not necessarily be the best response. For example, suppose that $m_{11} = 0$, while m_{01} and m_{10} are sufficiently large such that Eqs. (10) and (11) are satisfied (e.g., most friends use Windows or Mac OS, but none of them use both). Since $m_{11} = 0$, conditions (12) and (13) reduce to $m_{10}/k > c/b$ and $m_{01}/k > c/a$, respectively, and these conditions are also satisfied since Eqs. (10) and (11) hold for $m_{11} = 0$. Therefore, the best strategy turns out to be $s^* = 11$ (e.g., using both Windows and Mac), regardless of the fact that no neighbor adopts $s = 11$.

It is also straightforward to show that

$$v(01,\mathbf{m}) > v(10,\mathbf{m}) \quad \text{iff} \quad am_{01} - bm_{10} + (a-b)m_{11} > 0, \tag{14}$$

which suggests that a player's strategy may switch from 01 to 10 or vice versa in the process of diffusion, depending on the relative size of m_{01} and m_{10}. The diffusion process is thus generally non-monotonic, unlike the standard (irreversible) binary-state cascade models (Jackson, 2008; Morris, 2000; Unicomb et al., 2021; Watts, 2002).

2.2.3. *p-dominance and its relation to the threshold conditions*

In the previous subsection, we obtained the fractional threshold conditions for a strategy to be the best response. Here, we argue that a commonly used equilibrium selection criterion, *p-dominance* (Kajii and Morris, 1997; Morris et al., 1995), can be interpreted as a sufficient condition for the corresponding threshold condition.

Definition (Morris et al.1995, Kajii and Morris 1997)**.** *Let $\tilde{u}(s_i,s_j)$ denote the (i,j)th element of the payoff matrix, and let π on S be a probability distribution where $\sum_{s\in S}\pi(s) = 1$. The strategy pair (s_i,s_i) is p-dominant if for every probability distribution π on S such that $\pi(s_i) \geq p$, and for every $s_\ell \in S$,*

$$\sum_{s_j\in S}\pi(s_j)\tilde{u}(s_i,s_j) \geq \sum_{s_j\in S}\pi(s_j)\tilde{u}(s_\ell,s_j). \tag{15}$$

[6] If there are tie values (i.e., $v(s,\mathbf{m}) = v(s',\mathbf{m})$ for $s \neq s'$), we randomly select one strategy. If $k = 0$, however, we keep the original strategy to focus on the peer effect.

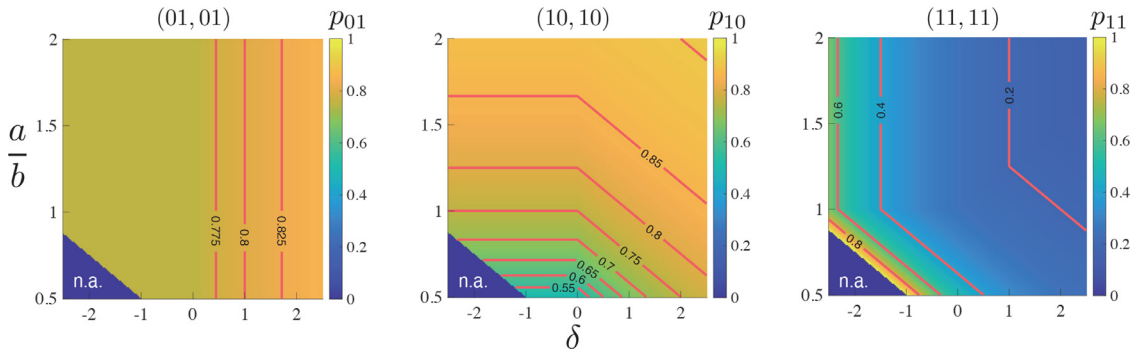

Fig. 2. Minimum values of p for a strategy pair to be p-dominant. We set $b = 4$ and $c = 1$, focusing on the parameter space in which $\delta > c - a$ and $\delta > c - b$.

A Nash equilibrium (s_i, s_i) is said to be p-dominant if s_i is a best strategy as long as the neighbors adopt strategy s_i with a probability greater than or equal to p. While p-dominance is originally an equilibrium characterization for games with incomplete information, this concept is closely related to the threshold conditions shown in the previous section. From Eqs. (10), (12) and (14), one can show that $s = 01$ will be the best response if the fraction of 01-neighbors, m_{01}/k, satisfies all of the following three conditions:

$$\frac{m_{01}}{k} > -\frac{m_{11}}{k} + \frac{c}{a}, \tag{16}$$

$$\frac{m_{01}}{k} > -\frac{a}{a+b}\frac{m_{11}}{k} + \frac{b}{a+b}, \tag{17}$$

$$\frac{m_{01}}{k} > \begin{cases} \frac{\delta}{b}\frac{m_{11}}{k} + 1 - \frac{c}{b}, & \text{if } \delta < 0, \\ -\frac{\delta}{b+\delta}\frac{m_{10}}{k} + 1 - \frac{c}{b+\delta}, & \text{if } \delta \geq 0, \end{cases} \tag{18}$$

where we used the inequality $m_{01} + m_{10} + m_{11} \leq k$. Now, consider more stringent conditions for which the inequalities (16)–(18) will hold for any configuration of $(m_{00}/k, m_{10}/k, m_{11}/k)$. Such conditions are given by

$$\frac{m_{01}}{k} > \frac{c}{a}, \quad \frac{m_{01}}{k} > \frac{b}{a+b}, \quad \frac{m_{01}}{k} > \begin{cases} 1 - \frac{c}{b} & \text{if } \delta < 0, \\ 1 - \frac{c}{b+\delta} & \text{if } \delta \geq 0. \end{cases} \tag{19}$$

The combined condition of (19) is thus a sufficient condition for $s = 01$ to be the best response. Indeed, the strategy pair (s, s) is p-dominant for any $p \in [p_s, 1]$ and $s \in S$ such that

$$p_{00} = \max\left\{\frac{a-c}{a}, \frac{b-c}{b}, 1 - \frac{2c}{a+b+\delta}\right\}, \tag{20}$$

$$p_{01} = \max\left\{\frac{c}{a}, \frac{b}{a+b}, 1 - \frac{c}{\max\{b, b+\delta\}}\right\}, \tag{21}$$

$$p_{10} = \max\left\{\frac{c}{b}, \frac{a}{a+b}, 1 - \frac{c}{\max\{a, a+\delta\}}\right\}, \tag{22}$$

$$p_{11} = \max\left\{\frac{2c}{a+b+\delta}, \frac{c}{b+\delta}, \frac{c}{a+\delta}\right\}. \tag{23}$$

Note that p_{01} is equivalent to the maximum threshold in (19). This implies that if the fraction m_{01}/k is interpreted as the probability of a randomly selected neighbor adopting $s = 01$ (i.e., $\pi(01)$), then p_{01} would coincide with the relevant threshold value in (19). This argument obviously holds true for the other strategies as well. Fig. 2 shows the values of p_s for different parameter combinations.

In Section 4, we calculate the dynamical paths for the aggregate share of each strategy. There, we will examine whether a strategy s would increase its popularity once its share exceeds p_s indicated in Fig. 2. If the probability distribution of neighbors' strategies is well approximated by the aggregate shares of each strategy in the population, then p-dominance would indeed become a sufficient condition for a strategy to be adopted by the majority of players in the steady state.

3. Analytical framework for describing the dynamics

In this section, present analytical approaches to describing the dynamics of diffusion. Throughout the analysis, we assume that strategy 00 is the status quo for all players, except for a certain fraction of players who are initially "active." Then, the neighbors of the initially active players (or the "seed players") may respond by adopting optimal strategies other than 00, which may initiate cascades through edges in the network.

Since the strategic choice of each player can be expressed as a function of the neighbors' profile $\mathbf{m}$, we introduce a probability $F_{\mathbf{m}}(s \to s')$ that strategy changes from s to s':[7]

$$F_{\mathbf{m}}\left(s \to s^{'}\right) = \begin{cases} 1 & \text{if } s^{'} = s^{*}(\mathbf{m}), \\ 0 & \text{otherwise.} \end{cases} \tag{24}$$

Note that the choice of a new strategy does not depend on the player's current strategy s. This indicates that, unlike the standard binary-state models (Morris, 2000; Watts, 2002), the strategic choice is fully reversible and is determined solely in response to the neighbors' profile $\mathbf{m}$. We also call $F_{\mathbf{m}}$ the *response function*.

In the next subsection, we explain an analytical method for calculating the fraction of players adopting a strategy as a solution of a system of differential equations. Throughout the paper, we employ the *approximate master equations (AMEs)* method, which is a more sophisticated version of the *mean-field (MF)* method. The difference between the AME and MF methods is discussed in Appendix A.

3.1. Approximate master equations

Let $\mathcal{V}^{s}_{|\mathbf{m}|=k}(t)$ denote the set of k-degree players that belong to the $(s, \mathbf{m})$ class at time t, i.e., all the players in $\mathcal{V}^{s}_{|\mathbf{m}|=k}$ adopt strategy $s \in S$ and have k neighbors. The fraction of k-degree players belonging to the $(s, \mathbf{m})$ class is given by

$$\rho^{s}_{k,\mathbf{m}}(t) \equiv \frac{|\mathcal{V}^{s}_{|\mathbf{m}|=k}(t)|}{q_k N}, \tag{25}$$

where $q_k N$ is the total number of players with degree k. Then, the expected fraction of players adopting strategy $s \in S$ (i.e., s-players) at time t is given as

$$\rho^{s}(t) = \sum_{k} q_k \sum_{|\mathbf{m}|=k} \rho^{s}_{k,\mathbf{m}}(t), \tag{26}$$

where $\sum_{|\mathbf{m}|=k}$ denotes the sum over $\mathbf{m} = (m_{00}, m_{01}, m_{10}, m_{11})$ such that $\sum_{s\in S} m_s = k$. Our interest in this section is to calculate the dynamical path of ρ^{s} for each strategy $s \in S$. To this end, we need to describe the dynamics of $\rho^{s}_{k,\mathbf{m}}$, which capture changes in the population in a given $(s, \mathbf{m})$ class.

There are four factors that change $\rho^{s}_{k,\mathbf{m}}$ over time. Players will *leave* the $(s, \mathbf{m})$ class if *i*) their strategy changes from s to $s'(\neq s)$, or *ii*) their neighbors' profile changes from $\mathbf{m}$ to $\mathbf{m}'(\neq \mathbf{m})$. On the other hand, players will newly *enter* the $(s, \mathbf{m})$ class if *iii*) the players' strategies shift from $s'(\neq s)$ to s, or *iv*) the neighbor profiles shift from $\mathbf{m}'(\neq \mathbf{m})$ to $\mathbf{m}$. To take into account all of these four factors that will affect the behavior of $\rho^{s}_{k,\mathbf{m}}$, we employ an approximate master equations (AMEs) approach (Fennell and Gleeson, 2019; Gleeson, 2011; 2013). The dynamics of $\rho^{s}_{k,\mathbf{m}}$ is given by the following differential equation:

$$\begin{aligned} \frac{d}{dt}\rho^{s}_{k,\mathbf{m}} = &- \overbrace{\sum_{s^{'}\neq s} F_{\mathbf{m}}\left(s \to s^{'}\right)\rho^{s}_{k,\mathbf{m}}}^{\text{i) Leave, } s\to} - \overbrace{\sum_{r\in S}\sum_{r^{'}\neq r} m_r \phi_s\left(r \to r^{'}\right)\rho^{s}_{k,\mathbf{m}}}^{\text{ii) Leave, } \mathbf{m}\to} \\ &+ \underbrace{\sum_{s^{'}\neq s} F_{\mathbf{m}}\left(s^{'} \to s\right)\rho^{s^{'}}_{k,\mathbf{m}}}_{\text{iii) Enter, } \to s} + \underbrace{\sum_{r\in S}\sum_{r^{'}\neq r} (m_{r^{'}}+1)\phi_s\left(r^{'} \to r\right)\rho^{s}_{k,\mathbf{m}-\mathbf{e}_r+\mathbf{e}_{r^{'}}}}_{\text{iv) Enter, } \to \mathbf{m}}, \end{aligned} \tag{27}$$

for all $s \in S$ and $\mathbf{m}$ such that $\sum_{s\in S} m_s = k \in \{1, \ldots, k_{\max}\}$. We assume that $\frac{d}{dt}\rho^{s}_{k,\mathbf{m}} = 0$ for $k = 0$, meaning that isolated players will not be influenced by other players. $\phi_s(r \to r')$ denotes the probability that a neighbor of an s-player changes the strategy from r to r' for $r, r' \in S$:

$$\phi_s(r \to r') = \frac{\sum_k q_k \sum_{|\mathbf{m}|=k} m_s \rho^{r}_{k,\mathbf{m}} F_{\mathbf{m}}(r \to r')}{\sum_k q_k \sum_{|\mathbf{m}|=k} m_s \rho^{r}_{k,\mathbf{m}}}, \tag{28}$$

where the denominator $\sum_k q_k \sum_{|\mathbf{m}|=k} m_s \rho^{r}_{k,\mathbf{m}}$ represents the expected number of (s)–(r) edges that connect s-players and r-players at a given point in time. The expected number of (s)–(r) edges that change to (s)–(r') in a small time interval dt

[7] Players' choice also depends on degree k in the coordination games, but the degree is directly obtained by $\mathbf{m}$ since $k = \sum_{s\in S} m_s$.

is then given as $\sum_k q_k \sum_{|\mathbf{m}|=k} m_s \rho^r_{k,\mathbf{m}} F_{\mathbf{m}}(r \to r')dt$. The probability of a (s)–(r) edge being changed to a (s)–(r') edge in the interval dt, denoted by $\phi_s(r \to r')dt$, is calculated as the ratio of the expected number of edges that changes from (s)–(r) to (s)–(r') and the expected number of (s)–(r) edges, which leads to Eq. (28).

The first and second terms in Eq. (27) respectively capture the aforementioned factors i) and ii). The first term captures the rate at which the strategy of a player in the $(s, \mathbf{m})$ class shifts from s to $s'(\neq s)$ in an infinitesimal time interval dt. Similarly, the second term denotes the rate at which the neighbors' profile differs from $\mathbf{m}$. The third and fourth terms correspond to the factors iii) and iv), respectively. The third term captures the rate at which the strategy of the $(s', \mathbf{m})$-class players changes from $s'(\neq s)$ to s. The fourth terms shows the rate that the neighbors' profile newly becomes $\mathbf{m}$. $\mathbf{e}_r$ denotes the 4×1 vector with 1 in the r-th element and 0 in the other elements. The expression $\mathbf{m} - \mathbf{e}_r + \mathbf{e}_{r'}$ thus represents the neighbor profile that has $m_{r'} + 1$ in the r'-th element and $m_r - 1$ in the r-th element. It should be noted that Eq. (27) describes the dynamics under asynchronous updates in which only a fraction dt of players can change their strategies in response to their neighbor profiles in a small time interval. Therefore, while the optimal strategy is given as a function of $\mathbf{m}$ (Eq. 9), the current strategy of a player does not necessarily have a one-to-one correspondence with $\mathbf{m}$ in the process of diffusion. s and $\mathbf{m}$ recover the one-to-one correspondence defined by Eq. (9) in the steady state at which players have no incentive to change their strategies, i.e., a Nash equilibrium.

The system of differential equations can be solved by providing initial values $\rho^s_{k,\mathbf{m}}(0)$ for all $s \in S$ and $\mathbf{m} \in \{\mathbf{m} : |\mathbf{m}| = k,\ k = 0, \ldots, k_{\max}\}$. The number of differential equations in the system is calculated as the total number of ways of picking k balls in an urn with replacement and without ordering. In the urn there are balls of four different colors, so the total number of color patterns when one picks k balls is given by $\binom{4+k-1}{k} = \binom{k+3}{k}$. Since a player selects one of the four strategies and the degree k ranges from 0 to $k_{\max}$, the total number of differential equations leads to $4\sum_{k=0}^{k_{\max}} \binom{k+3}{k}$.[8]

3.2. Dominant strategies in Nash equilibria

Let us examine how the steady state of diffusion processes is affected by the payoff parameters (a, b, c), substitutability parameter δ, and network connectivity z. Fig. 3a shows the cascade region calculated using the AME. We find that within the cascade region in which $1 - \rho^{00} > 0$, there are some distinct subregions characterized by different dominant strategies, where we define a dominant strategy as the strategy employed by more than 50% of players in the Nash equilibrium (Fig. 3a). For a given δ, the dominant strategy varies with the relative attractiveness, a/b, and the average degree, z.[9] When $\delta = 0$, for instance, strategy 01 (resp. strategy 10) prevails only when the payoff value a (resp. b) is relatively large. Which strategy dominates the others also depends strongly on the degree of substitutability δ. Intuitively, strategy 11 will be dominant in most of the cascade region when both activities are complements (Fig. 3a, *middle*), whereas either strategy 01 or 10 will be adopted when the two activities exhibit strong substitutability (Fig. 3a, *right*).

It should be noted that shifts in dominant strategies, or *phase transitions*, occur in a discontinuous manner at the boundary of the dominant regions (Fig. 3b). A small change in a parameter may cause the current dominant strategy to be discarded in favor of another. In the class of binary-state threshold models, the possibility of global cascades can arise only when the network connectivity (i.e., the average degree z) is neither too weak nor too strong, and the boundaries of the average degree at which phase transitions occur are called *critical points* (Gai and Kapadia, 2010; Watts, 2002). In our "multistate" cascade model, there are possibly six types of boundaries at which dominant strategies switch: (00,01), (00,10), (00,11), (01,10), (01,11), and (10,11). The critical points for these transition patterns are characterized not only by the network connectivity z, but also by the relative attractiveness a/b and the degree of substitutability δ.

3.3. (In)stability of diffusion dynamics and symmetry breaking

To describe the mechanics of diffusion dynamics using phase diagrams, here we employ the MF approach (42), assuming that networks are z-regular random graphs. Note that when the network is z-regular, we have $\rho^s_k(t) = \rho^s(t) = \omega^s(t)$ from Eqs. (26), (40) and (41), since $q_k = 1$ for $k = z$ and $q_k = 0$ otherwise. Thus, the system of MF equations consists of four equations for the four variables: $\rho^{00}(t)$, $\rho^{01}(t)$, $\rho^{10}(t)$ and $\rho^{11}(t)$. Note that since there is a constraint that $\sum_{s\in S} \rho^s(t) = 1$, we can focus on three of them by replacing ρ^{00} $(= \omega^{00})$ with $1 - \rho^{01} - \rho^{10} - \rho^{11}$. In the following analysis, we mainly describe the dynamics of ρ^{01}, ρ^{10} and ρ^{11}, where ρ^{00} is determined residually.[10]

Fig. 4 shows the (sliced) phase diagrams for the diffusion of neutral goods (i.e., $\delta = 0$) in the ρ^{01}–ρ^{10} plane. Note that the combination of (ρ^{01}, ρ^{10}) must lie within the feasible region $\{(\rho^{01}, \rho^{10}) : \rho^{01} + \rho^{10} + \rho^{11} \leq 1,\ \rho^s \in [0, 1]\}$ (shaded in

[8] We solve the system of differential equations using an ODE solver, `ode45`, for Matlab. Our Matlab code is based on the multi-state-SOLVER package available from `https://github.com/peterfennell/multi-state-SOLVER`.

[9] Fig. 3 a exhibits "asymmetric" cascade regions with respect to a/b since parameter b is fixed (at 4) while a varies. The likelihood that an activity will spread depends not only on the relative size of the payoff parameters a and b, but also on the cost parameter c. Note that fixing parameter b does not lose generality since changing a has the same effect on the diffusion of strategy 01 as changing b has on the diffusion of strategy 10 for a given c.

[10] We drop time subscript t for brevity.

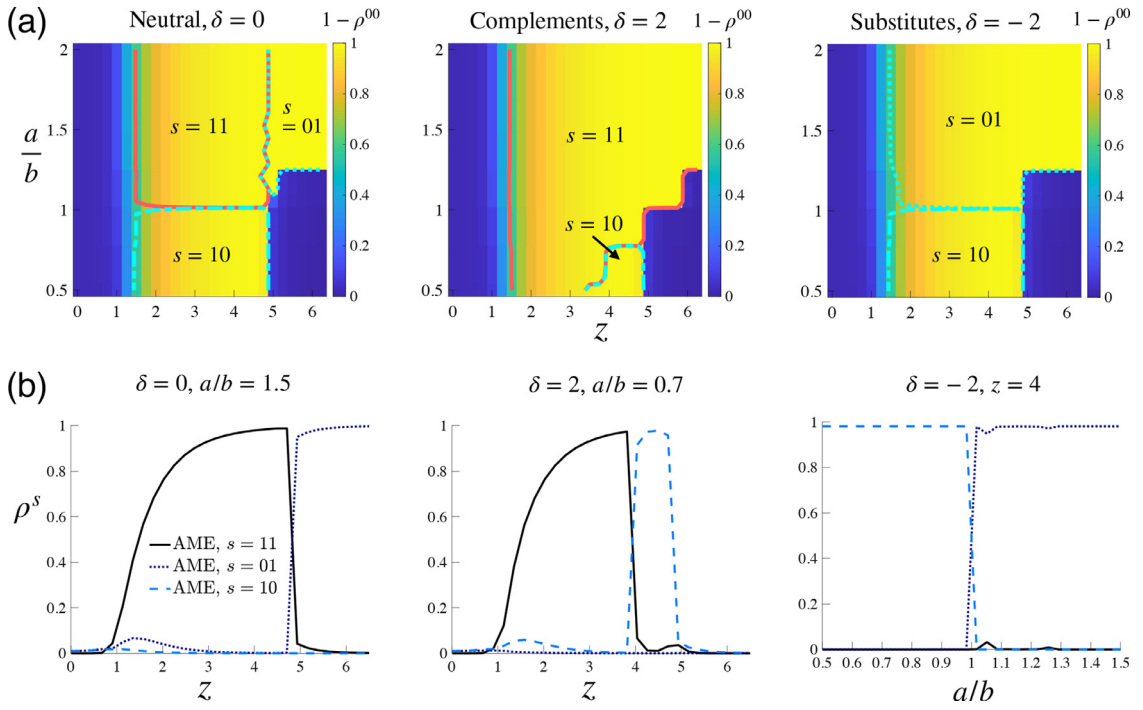

Fig. 3. Dominant strategy in Nash equilibrium. (a) Dominant strategy, which is a strategy employed by at least 50% of players, can be either 01 (light-blue dotted), 10 (light-blue dashed), or 11 (red solid). Color denotes $1-\rho^{00}(T)$ calculated by the AME. We use Erdős-Rényi networks with mean degree z. (b) Fraction of players adopting strategy s in the steady state. In both (a) and (b), we set $b = 4$, $c = 1$, $\rho_0^{01} = \rho_0^{10} = 0.01$, $\rho_0^{11} = 0$, and $T = 50$. (For interpretation of the references to color in this figure legend, the reader is referred to the web version of this article.)

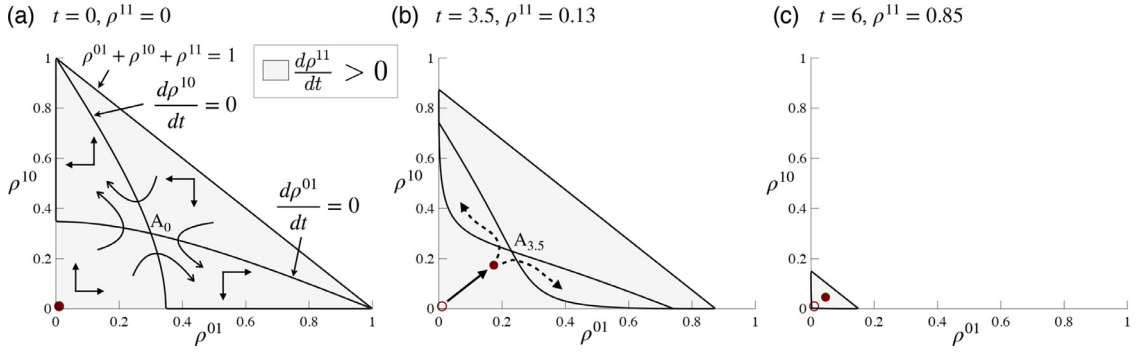

Fig. 4. Phase diagram for the diffusion of neutral activities ($\delta = 0$) obtained by the MF method using random 4-regular networks. Note that we have $d\rho^{11}/dt > 0$ independently of ρ^{01} and ρ^{10}, so that $\lim_{t\to\infty}\rho^{01}(t) = \lim_{t\to\infty}\rho^{10}(t) = 0$. Temporal symmetry breaking may occur since A_t is a saddle point. $a = b = 4$, $c = 1$, $\rho_0^{01} = \rho_0^{10} = 0.01$ and $\rho_0^{11} = 0$.

gray). The feasible region is divided into four subregions by the signs of the time derivatives $d\rho^{01}/dt$ and $d\rho^{10}/dt$ (denoted by arrows), which are calculated using Eq. (42) for a given $(\rho^{01}, \rho^{10}, \rho^{11})$. Suppose that the initial state is given by $(\rho^{01}(0), \rho^{10}(0), \rho^{11}(0)) = (0.01, 0.01, 0)$, which is denoted by the red circle in Fig. 4a. Since the time derivatives of ρ^{01} and ρ^{10} are both positive at the initial point, the combination (ρ^{01}, ρ^{10}) moves toward the saddle point A_0. Along with this, since $d\rho^{11}/dt > 0$, the feasible region shrinks as ρ^{11} increases with time. The closer the combination (ρ^{01}, ρ^{10}) is to the saddle point, the more likely it is that the symmetry between ρ^{01} and ρ^{10} will be broken (Fig. 4b). Note that while the theoretical path of (ρ^{01}, ρ^{10}) suggested by the MF equations approaches the saddle point, the actual (or simulated) path could deviate from the theoretical path because seed players are not necessarily located in symmetric positions. The extent to which a seed player affects the other players' behavior would depend not only on the number of their direct neighbors, but also on the number of neighbors at two or more steps away. Thus, there is no guarantee that the realized fraction of s-players is equal to the theoretical average ρ^s, as there are some fluctuations in the network structure that could not be captured by the current "average-based" approximation methods. If the realized path in a given network deviates from the MF path at least to some extent, then the subsequent path will move further away from the saddle point.

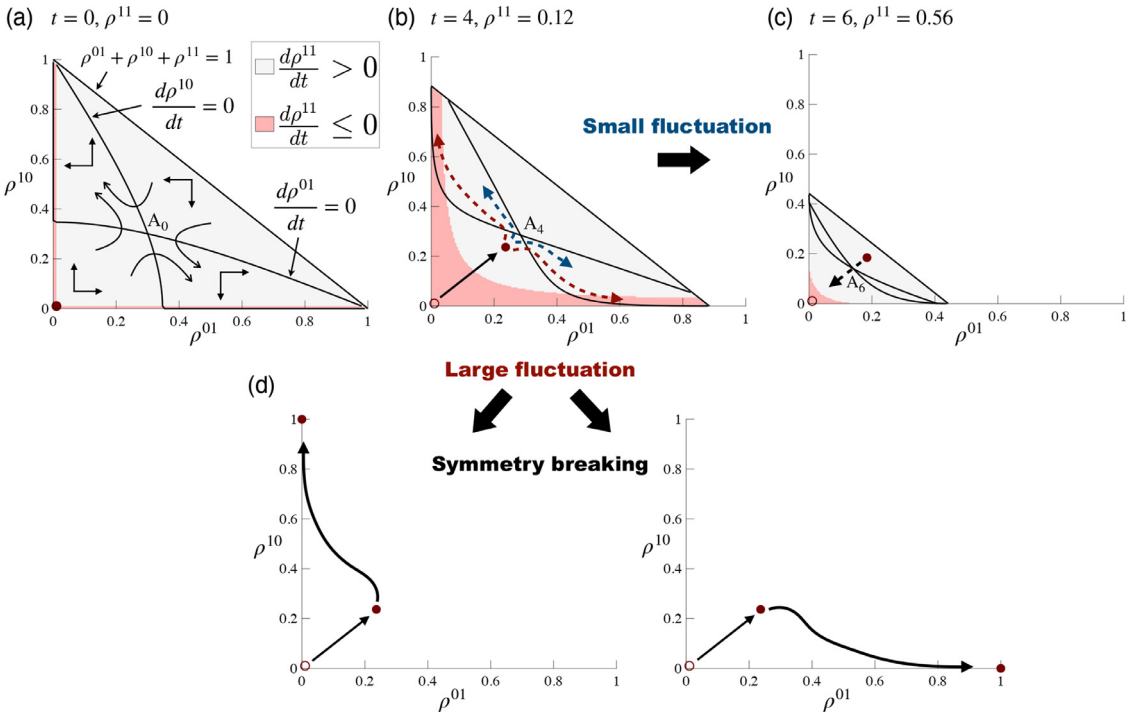

Fig. 5. Phase diagram for the diffusion of substitutes ($\delta = -2$) obtained by the MF method using random 4-regular networks. If the combination of (ρ^{01}, ρ^{10}) reaches the pale-red region in which $d\rho^{11}/dt < 0$, the feasible region of (ρ^{01}, ρ^{10}) expands, and the share of strategies approaches a stable state: $(\rho^{00}, \rho^{01}, \rho^{10}, \rho^{11}) = (0, 1, 0, 0)$ or (0,0,1,0). $a = b = 4$, $c = 1$, $\rho_0^{01} = \rho_0^{10} = 0.01$ and $\rho_0^{11} = 0$. (For interpretation of the references to color in this figure legend, the reader is referred to the web version of this article.)

However, because ρ^{11} is increasing, the feasible region continues to shrink, resulting in $\lim_{t\to\infty}\rho^{01}(t) = \lim_{t\to\infty}\rho^{10}(t) = 0$ and $\lim_{t\to\infty}\rho^{11}(t) = 1$ (Fig. 4c). This indicates that the observed symmetry breaking, if any, is transient, and strategy 11 will always be dominant in the steady state.

Fig. 5 illustrates the phase diagrams for substitutes ($\delta = -2$). We see that there is still a saddle point as seen in Fig. 4, but there arises a region in which $d\rho^{11}/dt < 0$ (shaded in pale red). In the diffusion of neutral activities, the feasible region always shrinks and thus any deviation from the theoretical path will be diminished, leading to the unique equilibrium $(\rho^{01}, \rho^{10}) = (0, 0)$. In the diffusion of substitutes, the same mechanics will still hold if the deviation from the MF path is not sufficiently large (Fig. 5c). However, the feasible region will expand if the deviation from the theoretical path is sufficiently large such that $d\rho^{11}/dt < 0$ (Fig. 5b). If this is the case, the observed symmetry breaking will no longer be a transient phenomenon, where the equilibrium for (ρ^{01}, ρ^{10}) will be given by (1,0) or (0,1) (Fig. 5d). In the following section, we will show that such a persistent symmetry breaking can indeed occur not only in z-regular random networks, but also in more complex Erdős-Rényi networks.

4. Quantitative analysis

4.1. Simulation procedure

To see how well the differential equations obtained by the AME (Eq. 27) and MF (Eq. 42) approaches capture the dynamics of diffusion, we compare the analytical results with simulated diffusion processes. We use Erdős-Rényi networks in the baseline analyses. The procedure of numerical simulation is as follows:

1. For a given z and N, generate an Erdős-Rényi network with connecting probability $q = z/(N-1)$.
2. Select seed players at random so that there are $\lfloor \rho_0^{01} N \rfloor$ players adopting strategy 01 and $\lfloor \rho_0^{10} N \rfloor$ players adopting strategy 10. The other players employ strategy 00 as the status quo.
3. Choose a fraction $dt \in (0, 1)$ of players uniformly at random and update their strategies to maximize their payoff v.
4. Repeat step 3 until convergence, where further updates would not change the strategy of any player.
5. Repeat steps 1–4.

To conduct simulations in a manner consistent with the continuous-time framework, we implement an asynchronous update in step 3, where a randomly chosen fraction dt of the players updates their strategies in an infinitesimally small interval dt (Gleeson, 2011; 2013). This is consistent with the AME and MF formulations because changes in the fraction $d\rho^s_{k,\mathbf{m}}$ in

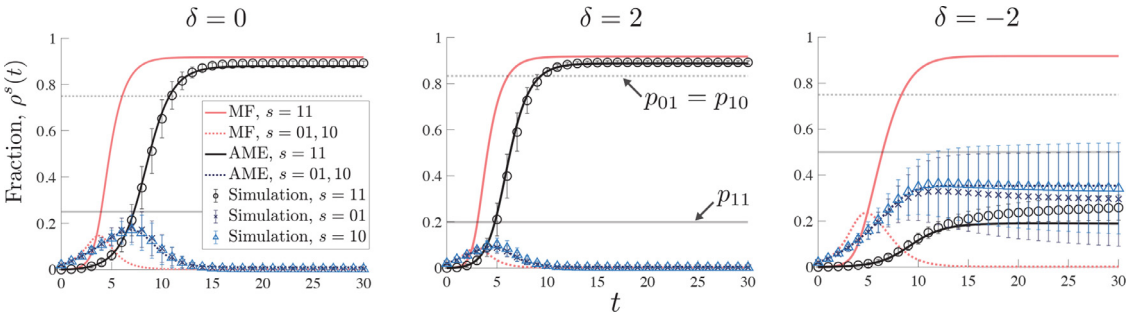

Fig. 6. Theoretical and simulation results for the path of $\rho^s(t)$. Symbols denote the averages over 100 runs on Erdős-Rényi networks with $z = 2.5$ and $N = 3000$. Error bar denotes one standard deviation. Horizontal dotted and solid gray lines respectively denote the values of p for (01,01) (or equivalently (10,10)) and (11,11) to be p-dominant. $a = b = 4$, $c = 1$, $\rho_0^{01} = \rho_0^{10} = 0.02$ and $\rho_0^{11} = 0$.

Eq. (27) (resp. $d\rho_k^s$ in Eq. 42) are explained by a fraction dt of the possible shifts in the players' states captured by the RHS of Eq. (27) (resp. Eq. 42). We set $dt = 0.01$ in all simulations. It should be noted that an asynchronous update could affect the simulated steady state because how and when symmetry breaking takes place would be influenced by small changes in the popularity of each strategy. In a model with a single activity (e.g., the Watts model), however, synchronous and asynchronous updating rules will yield the same steady state (Gleeson, 2008; Gleeson and Cahalane, 2007). In the model with two activities, both network structure and asynchronous updating become the source of randomness.

4.2. Dynamics of diffusion: symmetric payoffs

Let us consider the case of symmetric activities, where $a = b$ and $\rho^{01}(0) = \rho^{10}(0)$. Since $a = b$, the two activities A and B are equally attractive, so it is expected that $\rho^{01}(t) = \rho^{10}(t)$ for all t, other things being equal. We find that when the two activities are neutral ($\delta = 0$) or complements ($\delta > 0$), the path of $\rho^s(t)$ obtained by the AME method well matches the simulated path for any strategy s, while the MF approximation is generally less accurate (Fig. 6, *left* and *middle*). The standard deviations of the simulated $\rho^s(t)$ over 100 runs become vanishingly small as $t \to \infty$.

In contrast, when the two activities are substitutes ($\delta < 0$), the standard deviations of the simulated $\rho^s(t)$ increase over time, while the average values are still well approximated by the corresponding theoretical values obtained by the AME (Fig. 6, *right*). The discrepancy between theory and simulation observed in the propagation of substitutes reflects the fact that one of the two activities occasionally dominates the other even if the payoff parameters and the seed fractions are perfectly symmetric. This symmetry breaking occurs through the mechanism described in Section 3.3; when the activities are substitutable, players would not have an incentive to choose strategy 11, so once cascade occurs, either strategy 01 *or* 10 would prevail. The analytical solutions provide the existence of a symmetric equilibrium, but such an equilibrium would not be achieved in numerical simulations where players are connected in a heterogeneous way.

Fig. 6 also shows the values of p such that strategy pair (s_i, s_i) is p-dominant (denoted by p_{s_i} in Fig. 6, *middle*). As argued in Section 2.2.3, if the probability distribution of neighbors' strategies is approximated by the aggregate shares of each strategy, i.e., $\pi(s) \approx \rho^s$ for all $s \in S$, then p_{s_i} would be roughly interpreted as a (sufficient) threshold of ρ^{s_i} above which the strategy s_i will prevail. We see from Fig. 6 that in the cases of $\delta = 0$ and 2, in which $s = 11$ prevails, ρ^{01} does not exceed p_{01} while strategy 01 gains some extent of popularity in the early stage of the diffusion process. In contrast, ρ^{11} exceeds p_{11} and continue to gain popularity until it reaches the steady state. When $\delta = -2$, in contrast, no strategy exceeds the corresponding p.

Fig. 7a and 7b show the distributions of the difference $\rho^{01}(T) - \rho^{10}(T)$ for different values of δ. When the two activities are complements, we always have $\rho^{01}(T) = \rho^{10}(T)$ (Fig. 7a), in which case the AME solution is accurate for every instance of simulated contagion processes. In contrast, when they are substitutes, we have either $(\rho^{01}(T), \rho^{10}(T)) = (1, 0)$ or (0,1) in most of the simulation runs. This suggests that either activity A or B dominates with probability ≈ 0.5, depending on the details of the structure of the network that the analytical methods do not capture. Note that the AME solution will still describe the simulated equilibrium *on average*, but it does not necessarily mean that the AME solution is accurate for every instance of the propagation processes. In general, there is a negative relationship between δ and the standard deviation of $\rho^{01}(T) - \rho^{10}(T)$, and the essential result also holds true for random regular networks (Fig. 7c). On the other hand, when there is a certain extent of intrinsic asymmetry between the two activities (i.e., $a \neq b$), the AME method works quite well even for substitutable activities since symmetry breaking does not occur (see Appendix B).

5. Alternative model of diffusion

We have seen that players' interactions through 4×4 coordination games provide a mechanism by which an activity spreads over a network. To check the robustness of the results, here we consider an alternative model of diffusion in which players select their strategies to maximize utility functions.

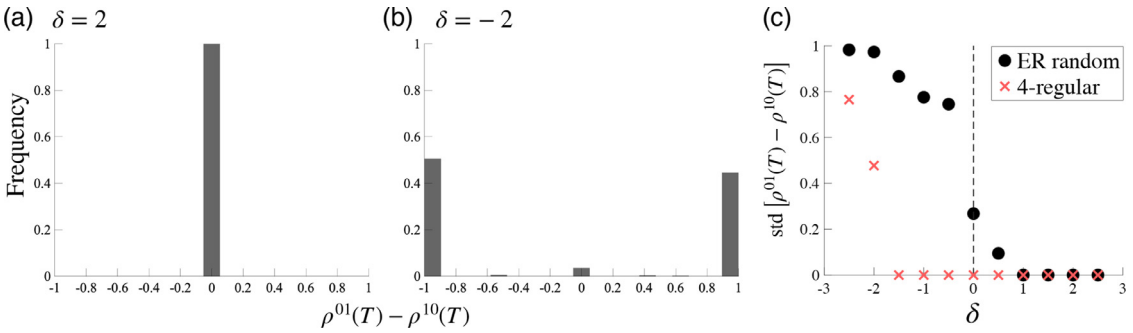

Fig. 7. Histogram of the difference $\rho^{01}(T) - \rho^{10}(T)$ for Erdős-Rényi networks with (a) $\delta = 2$ and (b) $\delta = -2$. Note that we always have $\rho^{01}(T) = \rho^{10}(T)$ when the activities are complements (i.e., $\delta = 2$), but when they are substitutes (i.e., $\delta = -2$), we have either $(\rho^{01}(T), \rho^{10}(T)) = (1, 0)$ or (0,1) in most of the 500 simulation runs. (c) Standard deviation of $\rho^{01}(T) - \rho^{10}(T)$ over 100 simulations. Black circle denotes the case of Erdős-Rényi random networks, and red cross denotes the case of random z-regular networks. In both panels, we set $z = 4$, $\rho_0^{01} = \rho_0^{10} = 0.01$, $\rho_0^{11} = 0$, $a = b = 4$, $c = 1$ and $T = 100$. (For interpretation of the references to color in this figure legend, the reader is referred to the web version of this article.)

Let $x_i^\ell \in \{0, 1\}$ denote player-i's binary action on activity $\ell \in \{A, B\}$. The strategy of player i is expressed by vector $\mathbf{x}_i = (x_i^A, x_i^B)$, and the strategies of the other players are summarized as $\mathbf{x}_{-i} = (x_1^A, x_1^B, \ldots, x_{i-1}^A, x_{i-1}^B, x_{i+1}^A, x_{i+1}^B, \ldots, x_N^A, x_N^B)$. Note that there is a one-to-one correspondence between $\mathbf{x}_i \in \{(0, 0), (0, 1), (1, 0), (1, 1)\}$ and $s_i \in \{00, 01, 10, 11\}$. Following Chen et al. (2018), we consider the following quadratic utility function:

$$u_i(s_i, s_{-i}) = \sum_{\ell=A,B} \left\{ \alpha^\ell x_i^\ell - \frac{1}{2}(x_i^\ell)^2 + \gamma \sum_{j \neq i} g_{ij} x_i^\ell x_j^\ell \right\} + \frac{1}{2}\beta x_i^A x_i^B \tag{29}$$

where $g_{ij} \in \{0, 1\}$ denotes the (i, j)th element of the adjacency matrix $\mathcal{G} = \left(g_{ij}\right)$; $g_{ij} = 1$ if there is an edge between i and j and $g_{ij} = 0$ otherwise. α^ℓ is a parameter that captures the benefit of enjoying an activity itself, which entails costs ($= 1/2$). γ and β respectively denote the benefit of cooperating with neighbors and the degree of substitutability. Thus, the larger β is the greater the complementarity between the two activities.

5.1. Absolute-threshold rules

The utility for each strategy is given by

$$u_i(00, s_{-i}) = 0, \tag{30}$$

$$u_i(01, s_{-i}) = \alpha^A - \frac{1}{2} + \gamma(m_{01} + m_{11}), \tag{31}$$

$$u_i(10, s_{-i}) = \alpha^B - \frac{1}{2} + \gamma(m_{10} + m_{11}), \tag{32}$$

$$u_i(11, s_{-i}) = \alpha^A + \alpha^B - 1 + \frac{\beta}{2} + \gamma(m_{10} + m_{01} + 2m_{11}). \tag{33}$$

Since the strategy of a player can be considered as a function of the neighbors' strategy profile $\mathbf{m} = (m_{00}, m_{01}, m_{10}, m_{11})^\top$, we can redefine the utility function as $\tilde{u}_i(s, \mathbf{m}) \equiv u(s, s_{-i})$. The optimal strategy is then given by

$$s^*(\mathbf{m}) = \arg\max_{s \in S} \tilde{u}(s, \mathbf{m}), \tag{34}$$

where we drop the subscript i for simplicity.

To analyze contagious effects, we impose the following assumptions:

Assumption 2. $\alpha^A \leq 1/2$, $\alpha^B \leq 1/2$, and $\alpha^A + \alpha^B - 1 + \beta/2 \leq 0$.

These assumptions guarantee that $\tilde{u}(s, (k, 0, 0, 0)^\top) \leq 0 \; \forall s \in S$, which prohibits players from adopting strategies other than 00 when no neighbors enjoy activities. This means that neighbors' influence is necessary for an activity to spread over the network. Since $\tilde{u}(00, \mathbf{m}) = 0$, a player selects a strategy other than 00 as long as the utility is positive.[11]

[11] If there are tie values (i.e., $\tilde{u}(s, \mathbf{m}) = \tilde{u}(s', \mathbf{m})$ for $s \neq s'$), we randomly select one strategy. If $\tilde{u}(s, \mathbf{m}) \leq 0$ for all $s \in S$, however, we select $s = 00$.

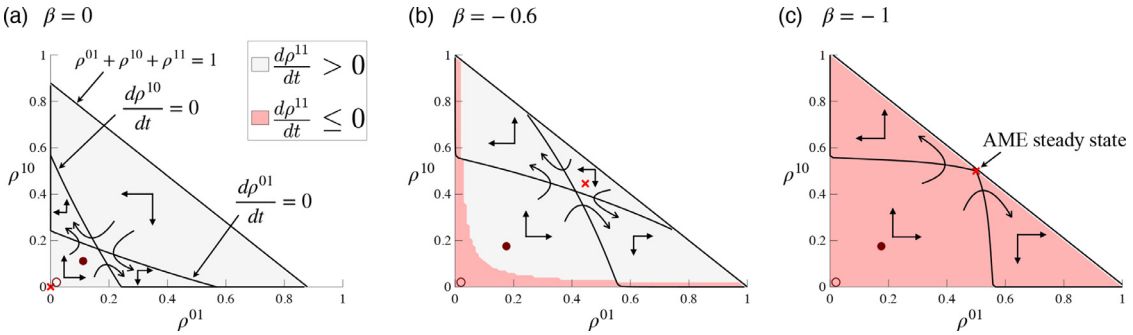

Fig. 8. Phase diagram of diffusion through utility-based games. Each panel shows a diagram at $t = 1$ based on random 4-regular networks with $\rho_0^{01} = \rho_0^{10} = 0.02$, $\rho_0^{11} = 0$, $\alpha^A = \alpha^B = 0.4$, and $\gamma = 0.2$. Red open and closed circles denote the initial and current points, respectively. Red cross denotes the steady state calculated by the AME.

The conditions for $\tilde{u}(01, \mathbf{m}) > 0$ and $\tilde{u}(10, \mathbf{m}) > 0$ are respectively given by the following threshold conditions:

$$\tilde{u}(01, \mathbf{m}) > 0 \quad \text{iff} \quad m_{01} + m_{11} > \frac{1}{\gamma}\left(\frac{1}{2} - \alpha^A\right), \tag{35}$$

$$\tilde{u}(10, \mathbf{m}) > 0 \quad \text{iff} \quad m_{10} + m_{11} > \frac{1}{\gamma}\left(\frac{1}{2} - \alpha^B\right). \tag{36}$$

The most important difference from the threshold conditions in coordination games, Eqs. (10) and (11), is that conditions (35) and (36) are independent of the player's degree k. This indicates that a player is more likely to join activity A as more neighbors join activity A, regardless of the fraction of active neighbors. This also implies that the larger the degree, the more likely it is for an activity to spread over a network. This type of diffusion has been studied within a class of *absolute-threshold models* (Granovetter, 1978; Karimi and Holme, 2013; Unicomb et al., 2021).

The conditions $\tilde{u}(11, \mathbf{m}) > \tilde{u}(01, \mathbf{m})$ and $\tilde{u}(11, \mathbf{m}) > \tilde{u}(10, \mathbf{m})$ are respectively rewritten as

$$\tilde{u}(11, \mathbf{m}) > \tilde{u}(01, \mathbf{m}) \quad \text{iff} \quad m_{10} + m_{11} > \frac{1}{\gamma}\left(\frac{1}{2} - \alpha^B - \frac{\beta}{2}\right), \tag{37}$$

$$\tilde{u}(11, \mathbf{m}) > \tilde{u}(10, \mathbf{m}) \quad \text{iff} \quad m_{01} + m_{11} > \frac{1}{\gamma}\left(\frac{1}{2} - \alpha^A - \frac{\beta}{2}\right), \tag{38}$$

Suppose for the moment that $\beta > 0$. Then Eq. (37) indicates that the threshold of the number of neighbors enjoying activity B $(= m_{10} + m_{11})$ above which strategy 11 is preferable to strategy 01 is smaller than that required for strategy 10 to be more preferable than 00 (Eq. 36). This is because when $\beta > 0$, the utility of enjoying both activities is greater than or equal to the sum of the utilities for each activity. However, if the two activities are substitutable (i.e., $\beta < 0$), the incentive to enjoy both activities is discouraged, so the condition for enjoying activity B *in addition to* A becomes more stringent than condition (36), which is the condition to enjoy activity B or do nothing. The same argument also holds for the relationship between $\tilde{u}(11, \mathbf{m})$ and $\tilde{u}(10, \mathbf{m})$ (Eq. 38).

Regarding the choice *between* the two activities, we have

$$\tilde{u}(01, \mathbf{m}) > \tilde{u}(10, \mathbf{m}) \quad \text{iff} \quad \alpha^A - \alpha^B + \gamma(m_{01} - m_{10}) > 0. \tag{39}$$

Whether this inequality holds depends on the relative number of active neighbors, $m_{01} - m_{10}$, which will be time-varying. Thus, a player's strategy may switch from 01 to 10 or vice versa in the process of diffusion, depending on the neighbors' status. Therefore, diffusion processes in this utility-based model are generally non-monotonic, similar to the contagion processes through coordination games.

5.2. Symmetry breaking

The previous MF and AME approaches can still be applied in this model by replacing the optimal strategy in the response function (24) with Eq. (34), which allows us to draw phase diagrams in the same way as before based on random regular networks (Fig. 8). Under our benchmark parameters $N = 3000$, $\rho_0^{01} = \rho_0^{10} = 0.02$, $\rho_0^{11} = 0$, $\alpha^A = \alpha^B = 0.4$, and $\gamma = 0.2$, we find that $d\rho^{11}/dt$ is always positive when the two activities are neutral (Fig. 8a), which causes the feasible region of (ρ^{01}, ρ^{10}) to shrink over time. Therefore, we will have $(\rho^{01}(T), \rho^{10}(T), \rho^{11}(T)) = (0, 0, 1)$ at the AME steady state when $\beta = 0$ (denoted by red cross).

On the other hand, as the substitutability parameter β becomes negative, there arises a wider region within which $d\rho^{11}/dt \leq 0$ (Fig. 8b and c). In particular, when $\beta = -1$, we see that $d\rho^{11}/dt$ is non-positive for the entire feasible region of

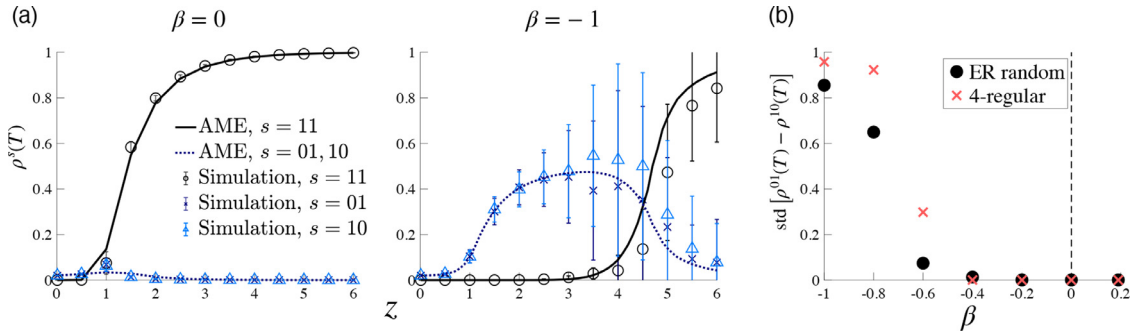

Fig. 9. Effect of substitutability on symmetry breaking in the model of utility-based games. (a) Steady-state fraction of strategy s against z for a given substitutability β in Erdős-Rényi networks. Error bars denote one standard deviations over 100 runs. (b) Relationship between the standard deviations of $\rho^{01}(T) - \rho^{10}(T)$ and β for $z = 4$, $N = 3000$, $\rho_0^{01} = \rho_0^{10} = 0.02$, $\rho_0^{11} = 0$, $\alpha^A = \alpha^B = 0.4$, $\gamma = 0.2$. T is set at 50 and 100 for panels (a) and (b), respectively.

(ρ^{01}, ρ^{10}). This suggests that the steady state obtained by the AME method is practically not attainable since any path deviating from the stable path (i.e., stable arm) would cause symmetry breaking, leading to $(\rho^{01}(T), \rho^{10}(T), \rho^{11}(T)) = (1, 0, 0)$ or (0,1,0). Again, this is a situation in which one of the activities would dominate the other purely by chance, depending on the realization of an instance drawn from an ensemble of random networks. When the degree of substitutability is moderate (Fig. 8b), there is a wide region of (ρ^{01}, ρ^{10}) in which $d\rho^{11}/dt > 0$, so the feasible region may shrink over time. This will make the upper bounds for ρ^{01} and ρ^{10} well below 1, resulting in a smaller degree of asymmetry compared to the case of $\beta = -1$.

Fig. 9a illustrates how the accuracy of the AME solutions is related to the degree of substitutability β and the average degree z. We find that when $\beta = -1$, each simulation run will be likely to deviate from the AME solution, while the average over multiple simulations appears to be close to the value predicted by the AME. These deviations from the AME values can be interpreted as an outcome of incidental diffusion due to symmetry breaking, whose dynamics are captured by the phase diagrams in Fig. 8c.

Naturally, we find that there is a negative relationship between the degree of substitutability β and the standard deviations of $\rho^{01}(T) - \rho^{10}(T)$ (Fig. 9b). When the two activities are strongly substitutable, it is highly likely that either of the two dominates the other (i.e., $\rho^{01}(T) = 1$ or $\rho^{10}(T) = 1$), resulting in the standard deviations being close to 1. When the substitutability is moderate, symmetry breaking still occurs, but the difference between $\rho^{01}(T)$ and $\rho^{10}(T)$ would be well below 1 because strategy 11 also prevails to some extent. In the phase diagram in Fig. 8b, this corresponds to an expansion of the area in which $d\rho^{11}/dt > 0$. In Section S2 in the Online Appendix, we present an analysis for the case of asymmetric preferences (i.e., $\alpha^A \neq \alpha^B$). Again, as in the model of coordination games, a lack of symmetry breaking generally improves the accuracy of the AME method.

So far, we have used synthetic networks in which nodes are sparsely and randomly connected, forming locally tree-like structures. To check the robustness of the observed results, we examined whether the AME method can predict the simulated diffusion processes on a finite-size empirical network in which the network structure is not necessarily tree-like (Section S3 in the Online Appendix). As an empirical network, we used an acknowledgment network collected from the papers published in *American Economic Review* in 2019–2020 (see, Section S3 for details). We find that the AME method still works well for the empirical network while the simulations are affected by a finite-size effect due to the small network size ($N = 447$).

6. Conclusion and discussion

We studied the dynamics of diffusion based on two different models of network games. In both models, we showed that the diffusion dynamics exhibit instability due to phase transitions and symmetry breaking. When the activities are complementary or neutral, the AME approach is highly accurate in predicting the popularity of each activity at any given point in time. However, when the activities are substitutable, "average-based" analytical equations such as MF and AME may not correctly describe the Nash equilibria attained in simulated propagation processes.

There are some issues to be addressed in future research. First, while we considered two activities and four pure strategies $\{00, 01, 10, 11\}$, one could extend the models to examine more than two activities since, in principle, the AME method can be applied to any number of states (or strategies) n. However, the difficulty is that the number of differential equations will increase to $n\sum_{k=0}^{k_{\max}} \binom{n+k-1}{k}$, so the computational cost would easily become prohibitive. For instance, if we have three types of activities and a degree distribution over $k = 0$ to 10, then the number of possible strategies is given by $n = 2^3$, and the number of differential equations will be $8\sum_{k=0}^{10} \binom{8+k-1}{k} = 350,064$. Second, it would be useful to introduce non-random structural properties, such as clustering and assortativity, which are frequently observed in real social

networks (Barabási, 2016; Newman, 2018). Since the AME system is already complex and there are a number of equations to be solved, introducing additional network properties would be a difficult task. Nevertheless, incorporating structural properties would be important not only to improve the accuracy of the AME running on real data, but also to enhance the predictability of diffusion. For example, firms would aim to enhance the popularity of new products through online social networks (Watts and Dodds, 2007), and governments may need to monitor the spread of misinformation and manipulations that could circulate through social media (Badawy et al., 2019). Third, it would also be useful to take into account the time-varying aspects of real-world networks. In many social networks, nodes and edges frequently appear and disappear, leading to changes in the network structure. The dynamic nature of networks has been extensively investigated within the framework of "temporal networks" in the field of network science (Holme and Saramäki, 2013). We hope that our study will stimulate further research in these directions.

Data availability

Data will be made available on request.

Appendix A. Mean-field approximation

In the AME approach, it is assumed that the transition rate of a neighbor's strategy, $\phi_s(r \to r')$, is independent of the states of the other neighbors, and their profile $\mathbf{m}$ is used to characterize each player's state. In the mean-field (MF) approach, we impose a stronger assumption that the strategies of neighbors are independent and randomly distributed following a multinomial distribution. Thus, the neighbor profile $\mathbf{m}$ is ignored and each player's state is characterized by a combination of strategy and degree, (s,k), rather than $(s,\mathbf{m})$.

To calculate the average fraction of players belonging to the (s,k) class, we define ρ_k^s as the sum of $\rho_{k,\mathbf{m}}^s$ over $\mathbf{m}$:

$$\rho_k^s(t) \equiv \sum_{|\mathbf{m}|=k} \rho_{k,\mathbf{m}}^s(t). \tag{40}$$

The average probability that a neighbor of a player adopts strategy $r \in S$, denoted by ω^r, is given by

$$\omega^r(t) \equiv \sum_{k\geq 1} \frac{kq_k}{z} \rho_k^r(t), \tag{41}$$

where kq_k/z is the probability that a randomly selected neighbor has degree k. The dynamics of ρ_k^s are then expressed as

$$\frac{d}{dt}\rho_k^s = -\sum_{s'\neq s} \rho_k^s \sum_{|\mathbf{m}|=k} \mathcal{M}_k(\mathbf{m},\boldsymbol{\omega}) F_{\mathbf{m}}\left(s \to s'\right) + \sum_{s'\neq s} \rho_k^{s'} \sum_{|\mathbf{m}|=k} \mathcal{M}_k(\mathbf{m},\boldsymbol{\omega}) F_{\mathbf{m}}\left(s' \to s\right), \tag{42}$$

where $\boldsymbol{\omega} \equiv (\omega^{00},\omega^{01},\omega^{10},\omega^{11})^\top$, and $\mathcal{M}_k(\mathbf{m},\boldsymbol{\omega})$ is the multinomial distribution:

$$\mathcal{M}_k(\mathbf{m},\boldsymbol{\omega}) \equiv \frac{k!}{m_{00}!m_{01}!m_{10}!m_{11}!} \left(\omega^{00}\right)^{m_{00}} \left(\omega^{01}\right)^{m_{01}} \left(\omega^{10}\right)^{m_{10}} \left(\omega^{11}\right)^{m_{11}}. \tag{43}$$

The first term in Eq. (42) captures the rate at which a player leaves the (s,k) class by changing the strategy from s to $s'(\neq s)$. The second term denotes the rate at which (s',k)-class players newly employ strategy s. Note that since we have four strategies and the degree ranges from 0 to $k_{\max}$, there are $4(k_{\max}+1)$ differential equations in the MF scheme, where $\frac{d}{dt}\rho_0^s = 0$.

Appendix B. Dynamics of diffusion: asymmetric payoffs

As we saw in Section 4.2, a symmetry-broken diffusion is occasionally observed when the degree of substitutability δ is low (Fig. 7), in which case the approximation methods do not accurately predict the path of simulated $\rho^s(t)$. However, when there is a certain extent of intrinsic asymmetry between the two activities, the AME method works quite well even for substitutable activities. If $a > b$, for example, activity A is always preferred to activity B, other things being equal, and accordingly the number of 10-players will be smaller than the number of 01-players. This makes it difficult to have a situation where the total payoff $v(10)$ is comparable to $v(01)$, which would be achieved if a certain fraction of neighbors adopt strategy 10. Thus, the unstable nature of diffusion process that we see for equally attractive activities would not materialize when the intrinsic attractiveness is different.

Fig. 10 shows the dynamical path of $\rho^s(t)$ when $a > b$ (The other parameters are the same as those in Fig. 6). When the activities are neutral ($\delta = 0$, Fig. 10, *left*), strategy 01 initially spreads to more than half of the players, and then most of the players begin to shift their strategies to $s = 11$, which leads to a decay in the fraction of 01-players. In the context of the phase diagram in Fig. 4, this corresponds to a situation where the feasible region $\rho^{01} + \rho^{10} + \rho^{11} \leq 1$ continues to shrink, and therefore ρ^{01} is bounded from above by $1 - \rho^{10} - \rho^{11}$. Note also that ρ^{01} does not exceed p_{01}, suggesting that (01,01) is not p-dominant.

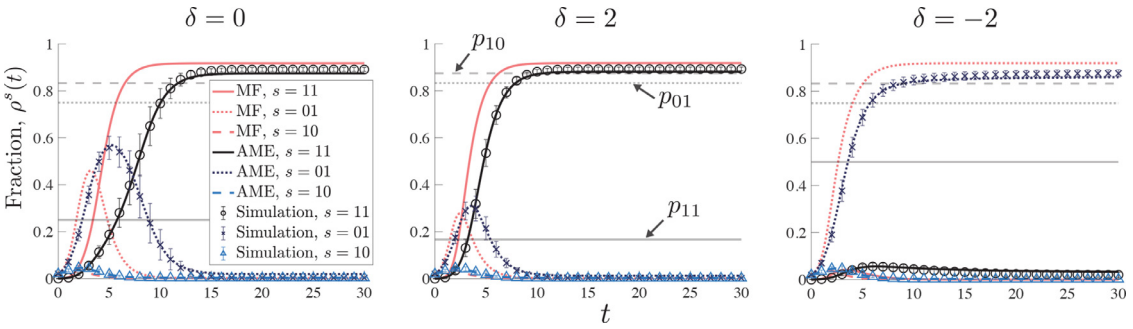

Fig. 10. Diffusion of asymmetric activities ($a = 6$ and $b = 4$). See caption of Fig. 6 for details.

When the activities are substitutes ($\delta < 0$), strategy 01 dominates the other strategies (Fig. 10, *right*). Since the total payoff of choosing activity B cannot be comparable to that of activity A in the process of diffusion, the simulated paths are quite stable over different runs, leading the standard deviations to be fairly small. Note that ρ^{01} surpasses p_{01} during the diffusion process, which implies that the strategy pair (01,01) is p-dominant.

Supplementary material

Supplementary material associated with this article can be found, in the online version, at 10.1016/j.jedc.2022.104561

References

Acemoglu, D., Robinson, J.A., Verdier, T., 2017. Asymmetric growth and institutions in an interdependent world. J. Politi. Econ. 125, 1245–1305.
Arigapudi, S., 2020. Transitions between equilibria in bilingual games under logit choice. J. Math. Econ. 86, 24–34.
Badawy, A., Lerman, K., Ferrara, E., 2019. Who Falls for Online Political Manipulation? In: Companion Proceedings of The 2019 World Wide Web Conference, pp. 162–168.
Ballester, C., Calvó-Armengol, A., Zenou, Y., 2006. Who's who in networks. wanted: the key player. Econometrica 74, 1403–1417.
Barabási, A.L., 2016. Network Science. Cambridge University Press, Cambridge.
Bonacich, P., 1987. Power and centrality: a family of measures. Am. J. Sociol. 92, 1170–1182.
Chatterjee, A., 2017. Endogenous comparative advantage, gains from trade and symmetry-breaking. J. Int. Econ. 109, 102–115.
Chen, Y.-J., Zenou, Y., Zhou, J., 2018. Multiple activities in networks. Am. Econ. J. Microecon. 10, 34–85.
Erdős, P., Rényi, A., 1959. On random graphs. Publicat. Math. 6, 290–297.
Fennell, P.G., Gleeson, J.P., 2019. Multistate dynamical processes on networks: analysis through degree-based approximation frameworks. SIAM Rev. 61, 92–118.
Gai, P., Kapadia, S., 2010. Contagion in financial networks. Proceed. Roy. Soc. A 466, 2401–2423.
Gleeson, J.P., 2008. Cascades on correlated and modular random networks. Phys. Rev. E 77, 046117.
Gleeson, J.P., 2011. High-accuracy approximation of binary-state dynamics on networks. Phys. Rev. Lett. 107, 068701.
Gleeson, J.P., 2013. Binary-state dynamics on complex networks: pair approximation and beyond. Phys. Rev. X 3, 021004.
Gleeson, J.P., Cahalane, D.J., 2007. An Analytical Approach to Cascades on Random Networks. SPIE Fourth International Symposium on Fluctuations and Noise, 66010W. International Society for Optics and Photonics.
Gleeson, J.P., Porter, M.A., 2018. Message-passing Methods for Complex Contagions. In: Lehmann, S., Ahn, Y.Y. (Eds.), Complex Spreading Phenomena in Social Systems. Springer, pp. 81–95.
Goyal, S., Janssen, M.C., 1997. Non-exclusive conventions and social coordination. J. Econ. Theory 77, 34–57.
Granovetter, M., 1978. Threshold models of collective behavior. Am. J. Sociol. 83, 1420–1443.
Harsanyi, J.C., Selten, R., 1988. A General Theory of Equilibrium Selection in Games. MIT Press, Cambridge.
Holme, P., Saramäki, J., 2013. Temporal Networks. Springer-Verlag, Berlin.
Immorlica, N., Kleinberg, J., Mahdian, M., Wexler, T., 2007. The role of compatibility in the diffusion of technologies through social networks. In: Proceedings of the 8th ACM Conference on Electronic Commerce, pp. 75–83.
Jackson, M.O., 2008. Social and Economic Networks. Princeton University Press, Princeton.
Jackson, M.O., Yariv, L., 2007. Diffusion of behavior and equilibrium properties in network games. Am. Econ. Rev. 97, 92–98.
Jackson, M.O., Zenou, Y., 2015. Games on networks. In: Handbook of Game Theory with Economic Applications 4. Elsevier, pp. 95–163.
Kajii, A., Morris, S., 1997. The robustness of equilibria to incomplete information. Econometrica 65, 1283–1309.
Karimi, F., Holme, P., 2013. Threshold model of cascades in empirical temporal networks. Physica A 392, 3476–3483.
Kobayashi, T., 2022. Diffusion dynamics of competing information on networks. Phys. Rev. E 106, 034303.
Kobayashi, T., Onaga, T., 2022. Dynamics of diffusion on monoplex and multiplex networks: a message-passing approach. Econ. Theory doi:10.1007/s00199-022-01457-x.
Kreindler, G.E., Young, H.P., 2014. Rapid innovation diffusion in social networks. Proceed. Natl. Acad. Sci. USA 111, 10881–10888.
Lelarge, M., 2012. Diffusion and cascading behavior in random networks. Games Econ. Behav. 75, 752–775.
López-Pintado, D., 2008. Diffusion in complex social networks. Games Econ. Behav. 62, 573–590.
López-Pintado, D., 2012. Influence networks. Games Econ. Behav. 75, 776–787.
Matsuyama, K., 2002. Explaining diversity: symmetry-breaking in complementarity games. Am. Econ. Rev. 92, 241–246.
Matsuyama, K., 2004. Financial market globalization, symmetry-breaking, and endogenous inequality of nations. Econometrica 72, 853–884.
Matsuyama, K., 2013. Endogenous ranking and equilibrium lorenz curve across (ex ante) identical countries. Econometrica 81, 2009–2031.
Molloy, M., Reed, B., 1995. A critical point for random graphs with a given degree sequence. Random Struct. Algor. 6, 161–180.
Morris, S., 2000. Contagion. Rev. Econ. Stud. 67, 57–78.
Morris, S., Rob, R., Shin, H.S., 1995. p-Dominance and belief potential. Econometrica 63, 145–157.
Newman, M., 2018. Networks, 2nd ed. Oxford University Press, Oxford.
Oyama, D., Takahashi, S., 2015. Contagion and uninvadability in local interaction games: the bilingual game and general supermodular games. J. Econ. Theory 157, 100–127.

Sadler, E., 2020. Diffusion games. Am. Econ. Rev. 110, 225–270.
Unicomb, S., Iñiguez, G., Gleeson, J.P., Karsai, M., 2021. Dynamics of cascades on burstiness-controlled temporal networks. Nat. Commun. 12, 1–10.
Watts, D.J., 2002. A simple model of global cascades on random networks. Proceed. Natl. Acad. Sci. USA 99, 5766–5771.
Watts, D.J., Dodds, P.S., 2007. Influentials, networks, and public opinion formation. J. Consum. Res. 34, 441–458.
Young, H.P., 1993. The evolution of conventions. Econometrica 61, 57–84.
Young, H.P., 2011. The dynamics of social innovation. Proceed. Natl. Acad. Sci. USA 108, 21285–21291.